Journal of Applied Mechanics and Technical Physics, Vol. 48, No. 4, pp. 486–491, 2007

TURBULENT FLOW PAST A TRANSVERSE CAVITY WITH INCLINED SIDE WALLS. 2. HEAT TRANSFER

A. Yu. D'yachenko, V. I. Terekhov, and N. I. Yarygina

UDC 536.24

Convective heat transfer in a transverse cavity with a small aspect ratio, angle of wall inclination $\varphi = 30$–$90°$, and heated bottom, frontal, and rear walls of the cavity is studied experimentally. Temperature distributions are measured in longitudinal and transverse sections on three walls; temperature fields are measured over the entire heated surface. Local and mean heat-transfer coefficients are calculated. The highest intensification of heat transfer is found to occur on the rear wall for low values of φ. Reconstruction of the one-cell structure to the two-cell structure of the primary vortex in the cavity leads to a drastic decrease in heat transfer over the cavity span from the end faces toward the center in the case with $\varphi = 60$ and $70°$. A certain increase in the mean heat-transfer coefficient averaged over the entire heated surface is noted for $\varphi = 60°$.

Key words: *turbulent flow, separated flow, boundary layer, cavity, vortex formation, heat transfer.*

Introduction. Results of studying the flow structure in the vicinity of the walls and distributions of pressure coefficients in the flow past cavities with inclined walls and with moderate aspect ratios are reported in [1]. The present paper describes the data on thermal characteristics and heat transfer in the same cavities with the angle of inclination of the side walls φ varied from 30 to 90°.

Heat transfer in rectangular cavities with different aspect ratios (ratios of the cavity width to its depth) was considered in some previous papers [2–13]. In [2–8], the length of the transverse cavity L was varied, and the Reynolds number was calculated by the formula $\mathrm{Re}_L = UL/\nu$, where U is the main flow velocity and ν is the kinematic viscosity. In [9], the varied parameter was the cavity depth H, and the governing Reynolds number was $\mathrm{Re}_H = UH/\nu$. As the parameter H/L in previous studies took different values, the generalizing relations for the mean Nusselt numbers were also different: $\langle \mathrm{Nu}_L \rangle \sim \mathrm{Re}_L^{0.5}$ [6], $\langle \mathrm{Nu}_L \rangle \sim \mathrm{Re}_L^{0.8}$ [3, 4], $\langle \mathrm{Nu}_H \rangle \sim \mathrm{Re}_H^{0.8}$ [9], and $\langle \mathrm{Nu}_L \rangle \sim \mathrm{Re}_L^{2/3}$ [2, 8].

It was shown [10–12] that the primary vortex does not occupy the entire volume of the cavity in extended rectangular cavities with $L/H \geqslant 2$, and the shear layer does not exert any significant effect on heat transfer. For fixed free-stream parameters, the mean Nusselt number $\langle \mathrm{Nu}_L \rangle = \langle \alpha \rangle L/\lambda$ is almost independent of the cavity width and substantially decreases with increasing cavity depth. The correlation dependence $\langle \mathrm{Nu}_H \rangle = \langle \alpha \rangle H/\lambda = f(\mathrm{Re}_H)$ is independent of the parameter H/L. In shallow transverse trenches, the dependence for a laminar boundary layer $\langle \mathrm{Nu}_H \rangle \sim \mathrm{Re}_H^{0.5}$ is valid for $\mathrm{Re}_H < 5 \cdot 10^4$ and the dependence for a turbulent boundary layer $\langle \mathrm{Nu}_H \rangle \sim \mathrm{Re}_H^{0.8}$ holds for $\mathrm{Re}_H > 5 \cdot 10^4$; in deep cavities ($H/L > 1$), the main exchange mechanism is turbulent diffusion, and the law $\langle \mathrm{Nu}_H \rangle \sim \mathrm{Re}_H^{2/3}$ is valid.

In various power-engineering facilities, the shape of transverse cavities may be different from a rectangle. The angle of inclination of the side walls may vary in a wide range. Practically no results on dynamic and thermal characteristics in such cavities are available, which makes solving this problem urgent. It was shown [10–12] that a change in the angle of inclination of the side walls from 45 to 90° exerts a significant effect on heat transfer. If the

Kutateladze Institute of Thermophysics, Siberian Division, Russian Academy of Sciences, Novosibirsk 630090; terekhov@itp.nsc.ru; yarygina@itp.nsc.ru. Translated from Prikladnaya Mekhanika i Tekhnicheskaya Fizika, Vol. 48, No. 4, pp. 23–29, July–August, 2007. Original article submitted April 24, 2006; revision submitted June 30, 2006.

angle between the side wall and the bottom is $\varphi = 60°$, the heat transfer from the cavity bottom becomes more intense; at $\varphi = 45°$, the transition from the laminar to the turbulent heat transfer is delayed. In those papers, however, heating of the cavity bottom only was considered, and heat transfer was measured only in the central cross section of the cavity. In the present paper, we expanded the range of the angles of inclination φ and examined heating of three walls (two side walls and bottom wall). In addition, heat transfer from the entire heated surface is measured by means of thermography.

Test Conditions. The experiments were performed in a wind tunnel based at the Institute of Thermophysics of the Siberian Branch of the Russian Academy of Sciences. The test channel of the wind tunnel had a cross section of 200×200 mm and a length of 1000 mm. The model with the cavity was placed on the bottom wall of the channel. There was a shield 480 mm long ahead of the cavity, and the length of the flat surface behind the cavity was 200 mm.

We studied the flow past a cavity of the following size: depth $H = 60$ mm, width of the cavity bottom $L = 60$ mm, length of the cavity in the transverse direction $S = 180$ mm, $S/H = 3$, and $H/L = 1$. The cavity walls were made of a cloth-laminate sheet 20 mm thick. The experiments were performed with angles of inclination of the side walls $\varphi = 30$, 45, 60, 70, 80, and 90°.

The measurements were performed for free-stream velocities $U = 5$–35 m/sec, which corresponded to Reynolds numbers $\mathrm{Re}_H = HU/\nu = 2 \cdot 10^4$–$1.4 \cdot 10^5$. For all free-stream velocities, the boundary layer ahead of the cavity was turbulent. The momentum thickness of the boundary layer prior to flow separation was $\delta^{**} = 3.2$–3.7 mm. The degree of free-stream turbulence in the channel stayed at the natural level and reached 1.5%.

The side walls and the cavity bottom were heated by a strip heater made of aluminum foil 0.36 μm thick with 5-mm-wide strips in the regime of a constant heat flux. The cavity surfaces contained 158 Chromel–Copel thermocouples in three longitudinal sections on the bottom, five longitudinal sections on the side walls, and four sections across the flow (one cross section on each side wall and two cross sections on the cavity bottom). Four thermocouples were placed on the back side of each heated wall to estimate the heat loss through the plate.

In experiments with thermography, the cavity with the heater was located on the side wall and was flush-mounted with the channel wall. The cavity was heated during 1 h in a necessary heating mode, after which the wall temperature was measured by a "Sova" infrared imager. The method of thermographic measurements of the temperature field was described in detail in [14]. As a result of scanning, a frame 192×192 pixels was formed. The temperature field was digitized, based on results of two or more thermocouples, and thermograms were constructed by special computer codes.

Test Results. Based on the thermocouple measurements and IR scanning of the wall temperature, we calculated the local heat-transfer coefficients:

$$\alpha_i = (q_w - \Delta q)/(T_{wi} - T_0).$$

Here q_w is the specific heat flux, Δq is the heat loss, T_0 is the free-stream temperature, and T_{wi} is the local temperature of the wall.

Typical distributions of the local heat-transfer coefficients α_i in the central cross section in the flow on the frontal and rear walls and on the cavity bottom are plotted in Fig. 1 for all examined values of φ. The abscissa axis is the current coordinate on each wall divided by the length l_i of the mid-line on this wall. The scatter of experimental points on the cavity bottom for different angles of wall inclination is small; some intensification of heat transfer is observed for $\varphi \leqslant 60°$, where the primary vortex decomposes into a two-cell structure [1]. At these angles, the flow in the cavity becomes essentially three-dimensional, and the vortex-formation process is similar to that in a hemispherical cavity [15]. On the frontal wall, the angle φ exerts a different effect on heat transfer: the heat transfer drastically decreases at $\varphi = 45°$ and even more significantly at $\varphi = 30°$. The heat transfer on the rear wall substantially increases with decreasing angle φ. The value of α_i near the bottom wall for $\varphi = 30$ and 45° is 1.7 times higher than that for $\varphi = 90°$. It is on the rear wall of the cavity where the highest heat-transfer intensity is reached.

Figure 2 shows the heat-transfer coefficients averaged over the mid-section length for each wall for different free-stream velocities in cavities with different angles of wall inclination. Naturally, the value of $\langle\alpha\rangle$ increases with increasing flow velocity. The heat transfer on the frontal wall reaches the maximum value at $\varphi = 60°$ at the moment of decomposition of the primary vortex on the cavity bottom into two vortices. The heat transfer on the bottom and on the rear wall decreases with increasing angle φ. The most significant decrease in the heat-transfer coefficient

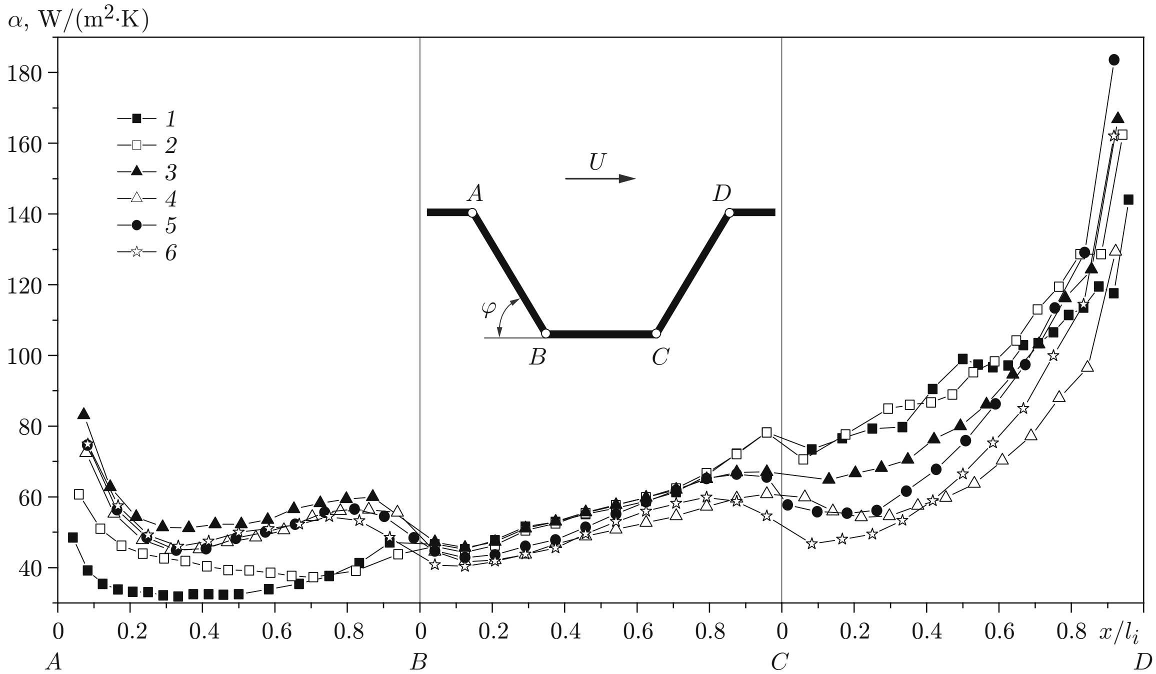

Fig. 1. Distribution of the local heat-transfer coefficient over the central cross section of the cavity for $\mathrm{Re}_H = 4 \cdot 10^4$: $\varphi = 30$ (1), 45 (2), 60 (3), 70 (4), 80 (5), and 90° (6).

is observed at $\varphi = 70°$, where the flow in the cavity becomes extremely unstable before reconstruction of the vortex structure. Such a behavior of the heat-transfer coefficient is associated with the emergence of the so-called elliptical instability induced by asymmetrically applied shear stresses [1]. The effect of flow instability is more pronounced at high free-stream velocities.

As the cavity flow is three-dimensional, the distributions of the coefficients α_i and $\langle\alpha\rangle$ over the central cross section do not give a comprehensive idea on heat transfer over the entire surface of the cavity. Figure 3 shows the distributions of the heat-transfer coefficients over the cavity span. On the frontal and rear walls, the sections with thermocouples were located at a distance of 35 mm from the upper edges. On the cavity bottom, two sections with thermocouples were located at a distance of 15 mm from the frontal and rear walls. It follows from Fig. 3 that the character of the spanwise distribution of the heat-transfer coefficient in the cavity for different values of φ is consistent with the topological pattern of vortex formation [1]. There is a fairly extended region on the frontal wall, where heat transfer depends weakly on φ for $\varphi = 60$–90°. In the cavity with small angles of inclination ($\varphi = 30$–45°), the heat-transfer intensity decreases by a factor of 1.45 and remains almost constant over the cavity span, except for regions close to the end faces. On the cavity bottom, at $\varphi = 70°$, the heat-transfer coefficient drastically decreases from the end faces toward the center when the opposing flow arises, and there is a minimum of α in the center. It should be noted that a similar effect was observed in [1] for the pressure coefficient. A decrease in heat transfer toward the center is also observed for $\varphi = 60$ and 80°, but in this case there are moderate-size regions with a constant heat-transfer coefficient in the central part of these regions. The character of the spanwise distributions on the rear wall remains unchanged. The heat-transfer coefficient substantially increases with decreasing angle φ and, correspondingly, with increasing angle of cavity expansion.

Based on the temperature fields obtained by thermography and thermocouple measurements, we calculated the surface-averaged heat-transfer coefficient and the corresponding Nusselt numbers Nu_H. For $\varphi = 90°$, the averaged results obtained by two methods for the cavity bottom are in good agreement. For high values of φ, however, the averaged results of IR imaging on the frontal and rear surfaces, however, are significantly different from the data of thermocouple measurements; hence, we averaged the thermocouple measurements over all sections to construct Figs. 4–6.

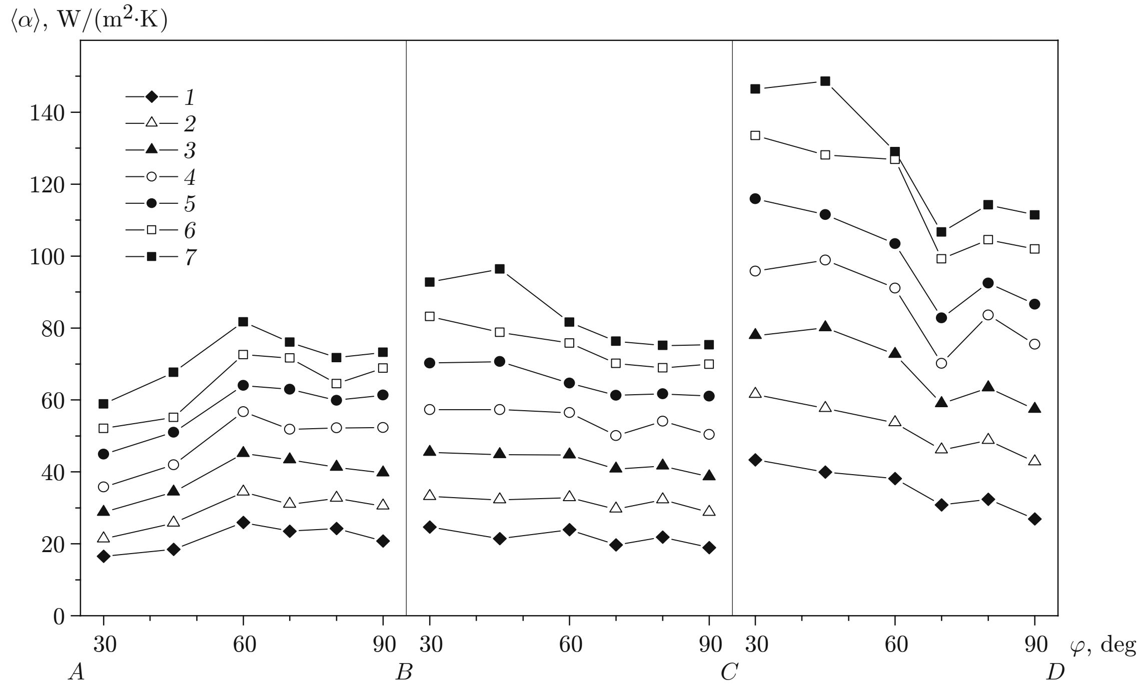

Fig. 2. Heat-transfer coefficient averaged over the mid-section length versus the angle of wall inclination φ: $U = 5$ (1), 10 (2), 15 (3), 20 (4), 25 (5), 30 (6), and 35 m/sec (7).

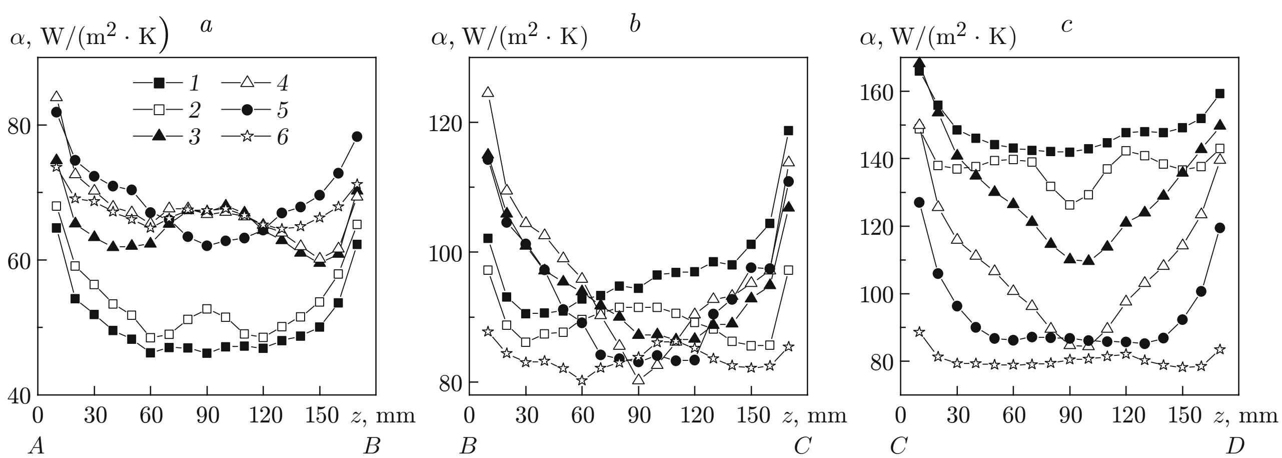

Fig. 3. Distribution of the local heat-transfer coefficient in cross sections over the cavity span for $U = 30$ m/sec and different angles φ: (a) frontal wall; (b) bottom; (c) rear wall; notation the same as in Fig. 1.

Figure 4 shows the Nusselt number $\langle \mathrm{Nu} \rangle$ averaged over the entire heated surface as a function of the Reynolds number Re_H for different angles φ. The dependence $\mathrm{Nu}_H \sim \mathrm{Re}_H^{2/3}$ typical of separated flows is valid for all angles, beginning from $\mathrm{Re}_H = 4 \cdot 10^4$. For strongly expanded cavities with $\varphi = 30$ and $45°$ and velocities $U = 5$–10 m/sec, the heat transfer corresponds to a laminar flow, and its behavior is caused by specific features of the flow on the frontal wall. It is the laminar character of the flow at these angles that is responsible for the decrease in the local heat-transfer coefficient on the frontal wall (see Fig. 1). The distribution of the mean Nusselt number averaged over the entire cavity surface is plotted in Fig. 5 versus the angle of inclination of the side walls. A certain increase in the mean heat-transfer coefficient can be noted for $\varphi \leqslant 60°$, but the highest value of $\langle \mathrm{Nu} \rangle$ is observed at $\varphi = 60°$, when a two-cell structure emerges. Actually, the mean Nusselt number depends only weakly on the angle of inclination of the side walls.

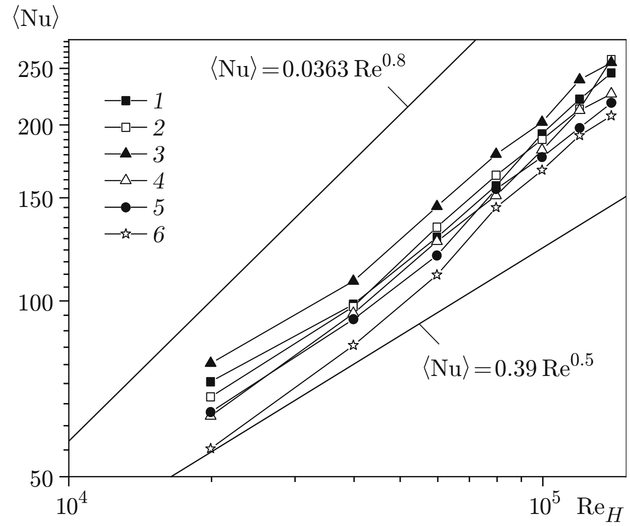

Fig. 4. Mean Nusselt number averaged over the entire heated surface versus the Reynolds number for different angles φ (notation the same as in Fig. 1).

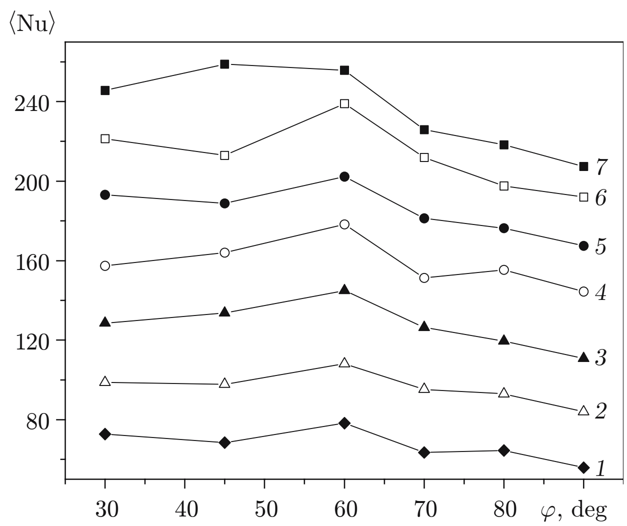

Fig. 5

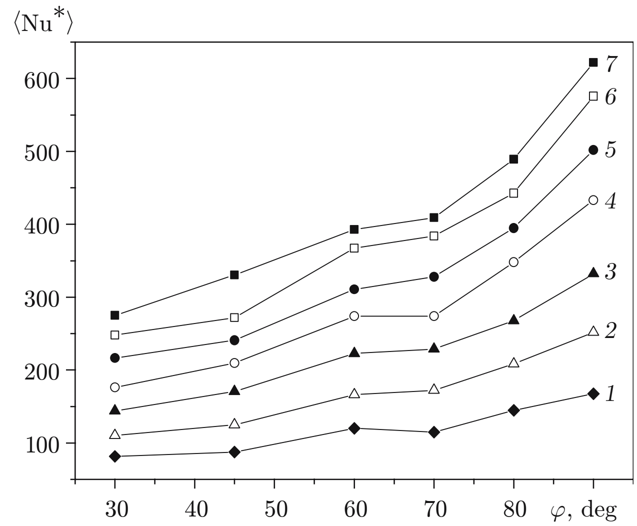

Fig. 6

Fig. 5. Mean Nusselt number averaged over the entire heated surface versus the angle φ for different flow velocities (notation the same as in Fig. 2).

Fig. 6. Mean Nusselt number determined over the interface between the cavity and external flow versus the angle φ for different flow velocities (notation the same as in Fig. 2).

The overall intensification of heat transfer in the cavity, however, is determined by the mean value $\langle\alpha\rangle$ calculated over the interface between the cavity and external flow rather than the heat-transfer coefficient averaged over the entire heated surface. Figure 6 shows the Nusselt number over this interface versus the angle φ for different velocities of the main flow. As the angle of wall inclination decreases, the area of the interface increases; correspondingly, the mean Nusselt number decreases. It can be noted, nevertheless, that the dependence $\langle \mathrm{Nu} \rangle = f(\varphi)$ is nonmonotonic, which is caused by certain local intensification of heat transfer at $\varphi = 60°$ and a small decrease in heat transfer at $\varphi = 70°$. Heat transfer behind the transverse cavity requires further study. By analogy with hemispherical cavities [15], heat transfer at a distance equal to the cavity depth behind cavities with large angles of expansion is expected to become more intense owing to self-sustained oscillations of the two-cell vortex structure of the cavity flow. An interesting problem is also the effect of high external turbulence on heat transfer in a cavity with inclined side walls. Some recent results [13] revealed an increase in heat transfer in the cavity up to 40% for 15% turbulence of the main flow, which is significantly greater than the heat transfer behind a rib or a step.

Conclusions. Heat transfer in a transverse cavity with a moderate aspect ratio ($S/H = 3$) and with angles of inclination of the side walls $\varphi = 30$, 45, 60, 70, 80, and 90° is studied in the range of Reynolds numbers $\mathrm{Re}_H = 2 \cdot 10^4$–$1.4 \cdot 10^5$. Local heat-transfer coefficients on three walls in the central section and in spanwise sections of the cavity are measured. It is shown that the heat-transfer coefficient substantially increases on the rear wall with decreasing angle φ. In the case of flow reconstruction at $\varphi = 60$ and 70° and emergence of the opposing flow, the distribution of the heat-transfer coefficient over the cavity span displays a drastic decrease in the cavity center. A certain increase in the heat-transfer coefficient averaged over the entire heated surface at $\varphi = 60°$ is noted.

This work was supported by the Russian Foundation for Basic Research (Grant Nos. 04-02-16070 and 06-08-00300).

REFERENCES

1. A. Yu. D'yachenko, V. I. Terekhov, and N. I. Yarygina, "Turbulent flow past a transverse cavity with inclined side walls. 1. Flow structure," *J. Appl. Mech. Tech. Phys.*, **47**, No. 5, 671–678 (2006).
2. A. F. Charwat, C. F. Dewey, J. N. Roos, and J. A. Hitz, "An investigation of separated flows. 1. Flow in the cavity and heat transfer," *J. Aerospace Sci.*, **8**, No. 7, 513–527 (1961).
3. R. A. Seban, "Heat transfer and flow in a shallow rectangular cavity with subsonic turbulent air flow," *Int. J. Heat Mass Transfer*, No. 8, 1353–1358 (1965).
4. J. Fox, "Heat transfer and air flow in a transverse rectangular ditch," *Int. J. Heat Mass Transfer*, No. 7, 269–279 (1965).
5. R. L. Haugen and A. M. Dhanak, "Heat transfer in turbulent boundary-layer separation over a surface cavity," *Trans. ASME, J. Heat Transfer*, **89**, No. 4, 335–340 (1967).
6. H. Yamamoto, N. Seki, and S. Fukusako, "Forced convection heat transfer on heated bottom surface of a cavity," *Trans. ASME, J. Heat Transfer*, **101**, No. 3, 112–117 (1979).
7. V. V. Degtyareva, V. A. Mukhin, and V. E. Nakoryakov, "Experimental study of mass transfer in axisymmetric cavities," *Inzh.-Fiz. Zh.*, **43**, No. 2, 181–186 (1982).
8. M. Hiwada, I. Mabuchi, and M. Kumada, "Three-dimensional flow and heat transfer in a rectangular cavity," *Heat Transfer Jpn. Res.*, **14**, No. 1, 75–96 (1985).
9. F. R. Richards, M. F. Young, and J. C. Haiad, "Turbulent forced convection heat transfer from a bottom heated open surface cavity," *Int. J. Heat Mass Transfer*, **30**, No. 11, 2281–2287 (1987).
10. V. I. Terekhov and N. I. Yarygina, "Forced-convection heat transfer from the bottom of trenches with rectangular or inclined walls," *Exp. Heat Transfer*, **9**, 133–148 (1996).
11. V. I. Terekhov and N. I. Yarygina, "Heat-transfer laws in cavities exposed to a turbulent flow," *Prom. Teplotekh.*, **19**, Nos. 4/5, 133–148 (1997).
12. V. I. Terekhov, S. P. Tret'yakov, and N. I. Yarygina, "Convective heat transfer from the bottom of cavities of different geometries," in: *Forced Convection of Single-Phase Fluid* [in Russian], Proc. 1st Russian National Conf. on Heat Transfer (Moscow, November 21–25, 1994), Vol. 1, Moscow Energy Inst., Moscow (1994), pp. 256–261.
13. V. I. Terekhov and N. I. Yarygina, "Heat transfer in separation regions of turbulized flows," in: *Forced Convection of Single-Phase Fluid*, Proc. 2nd Russian National Conf. on Heat Transfer (Moscow, October 26–30, 1999), Vol. 2, Moscow Energy Inst., Moscow (1998), pp. 244–247.
14. O. A. Kabov, I. V. Marchuk, and V. M. Chupin, "Thermal imaging study of the liquid film flowing on vertical surface with local heat source," *Russian J. Eng. Thermophys.*, **6**, No. 2, 104–138 (1996).
15. V. I. Terekhov and S. V. Kalinina, "Flow structure and heat transfer in the flow past a single spherical cavity," *Teplofiz. Aéromekh.*, **9**, No. 4, 497–520 (2002).